Supplementary Information

Dual-Interface Engineered SnO_2/Sn_4P_3@C Heterojunctions: Built-In Electric Field Driven LiF-Rich SEI and Ultrafast Kinetics for Highly Reversible Lithium Storage

Zhiqiang Huang [a], Zhilong Wu [a, c], Wenyi Miao [a], Zhongfen Yu [a], Hai Jia [b], Quanlin Chen [a], Xiaohui Huang [a], Zhiya Lin [b**], Shaoming Ying [a*]

[a] *College of New Energy and Materials, Ningde Normal University, Fujian Provincial Key Laboratory of Featured Materials in Biochemical Industry, Ningde 352100, China.*

[b] *College of Mathematics and Physics, Ningde Normal University, Ningde, 352100, China.*

[c] *College of Chemistry, Fuzhou University, Fuzhou 350002, China*

*Corresponding author:

Shaoming Ying E-mail: yingshaoming@126.com

Zhiya Lin E-mail: 1284555077@qq.com

Experimental section

2.1 Synthesis of SnO_2@C precursor

The SnO_2@C precursor was synthesized following a previously reported method with minor modifications[1]. Typically, $SnCl_4 \cdot 5H_2O$ (4.41 g), glucose (11.89 g), and HCl (0.85 mL, 12 mol·L^{-1}) were dissolved in 60 mL of distilled water. The solution was then transferred to a 100 mL Teflon-lined autoclave and heated at 180°C for 12 h to obtain a brown precipitate. After centrifugation and multiple washings with distilled water, the brown precipitate was dried at -60°C for 48 h using lyophilization. Subsequently, the product was annealed in a tube furnace at 500°C for 4 h under an Ar atmosphere to yield the final product, SnO_2@C, denoted as SOC.

2.2 Synthesis of SnO_2/Sn_4P_3@C composites

Typically, 0.1 g SOC (SnO_2@C) was hand-milled with 0.35 g $NaH_2PO_2 \cdot H_2O$ (Analytically pure) to ensure homogeneity. And then this blend was placed into a specially designed quartz tubde and heated at 280°C for 30 min with a ramping rate 2°C min^{-1} in Ar atmosphere. After the furnace cooled down, the dark sample was obtained by washing the mixtures with water and HCl solution (0.1 M) for several times, respectively. Finally, the product was dried at 60°C in a vacuum oven for 12 h. Finally, the product was dried at 80°C for 24 h to obtain the SnO_2/Sn_4P_3@C composite, denoted as SOPC. For comparative analysis, we meticulously adjusted the quantity of $NaH_2PO_2 \cdot H_2O$ (0.7 g) and

employed the aforementioned methods to achieve complete phosphorization of the SOC, thereby yielding Sn_4P_3@C composite, denoted as SPC.

2.3 Materials characterization

The morphological characteristics of the as-synthesized products were examined utilizing a field emission scanning electron microscope (FE-SEM, Hitachi SU8010) and a transmission electron microscope (TEM, FEI Talos F200x), both equipped with an energy dispersive X-ray spectrometer (EDX) and selected area electron diffraction (SAED) capabilities. The phase and chemical composition were determined through X-ray diffraction analysis (XRD, Bruker D8−DISCOVER, utilizing Cu Kα radiation, λ = 0.15406 nm) and X-ray photoelectron spectroscopy (XPS, Thermo Scientific K-Alpha+). The weight percentages of the products were ascertained via thermogravimetric analysis (TG-DSC, STA 409 PC, NETZSCH), conducted at a heating rate of 10°C per minute in an air atmosphere. The Brunauer-Emmer-Teller (BET) surface areas were calculated using a Belsorp max instrument (ASAP 2460). The Thermo Scientific Nicolet iS10 instrument obtained Fourier transform infrared (FT-IR) spectra.. The electronic properties of the SOC, SOPC, and SPC electrodes were further elucidated by ultraviolet photoelectron spectroscopy (UPS, Thermo Fisher Scientific escalab 250xi, He-I α = 21.22

eV). Calibration of binding energy values for XPS and UPS was achieved by referencing the Au 4f7/2 peak at 84.0 eV and the Fermi edge at 0 eV on a clean gold surface, respectively.

2.4 Cell fabrication and characterization

Electrochemical measurements were carried out using CR2025 coin cells. The working electrodes were prepared by coating homogeneous slurries containing as-synthesized active materials (SOC, SOPC and SPC), black carbon and poly(vinylidene fluoride) (Aldrich) at a mass ratio of 80:10:10 in N-methylpyrrolidone. The slurries were uniformly coated onto a 10 μm thick copper foil with a mass loading of 1−1.2 $mg \cdot cm^{-2}$ and then heated at 90°C for 12 h in a vacuum oven. The electrodes were pressed and die-cut into round disks with a diameter of 12 mm. Coin-type cells were assembled in an Ar-filled glove box with lithium metal foil as the counter electrode and a microporous polymer separator (Celgard2300, Celgard, Korea). The electrolyte used was 1 $mol \cdot L^{-1}$ $LiPF_6$ in ethylene carbonate/diethyl carbonate/dimethyl carbonate (1:1:1 by volume) with 10 vol% vinylene carbonate (VC). The charge/discharge measurements were performed using a battery test system (LAND CT3002A, Wuhan LAND Electronics. Ltd.) over a voltage range from 0.005 to 3.00 V *vs* Li/Li^+ at room temperature. Cyclic voltammetry (CV) and electrochemical impedance spectral (EIS) measurements were conducted on the CHI710E

electrochemical workstation. The CV measurements were carried out at a scan rate of 0.1 mV s^{-1}, ranging from 0.01 to 3.0 V. The EIS measurements were performed in a wide frequency range of 0.01 Hz ~ 100 kHz.

Reference:

[1] Huang, Z. Q.; Gao, H. Y.; Ju, J.; Yu, J. G.; Kwon, Y. U.; Zhao, Y. N. Sycamore-fruit-like SnO_2@C nanocomposites: Rational fabrication, highly reversible capacity and superior rate capability anode material for Li storage. *Electrochim. Acta* **2020**, *331*, 135297.

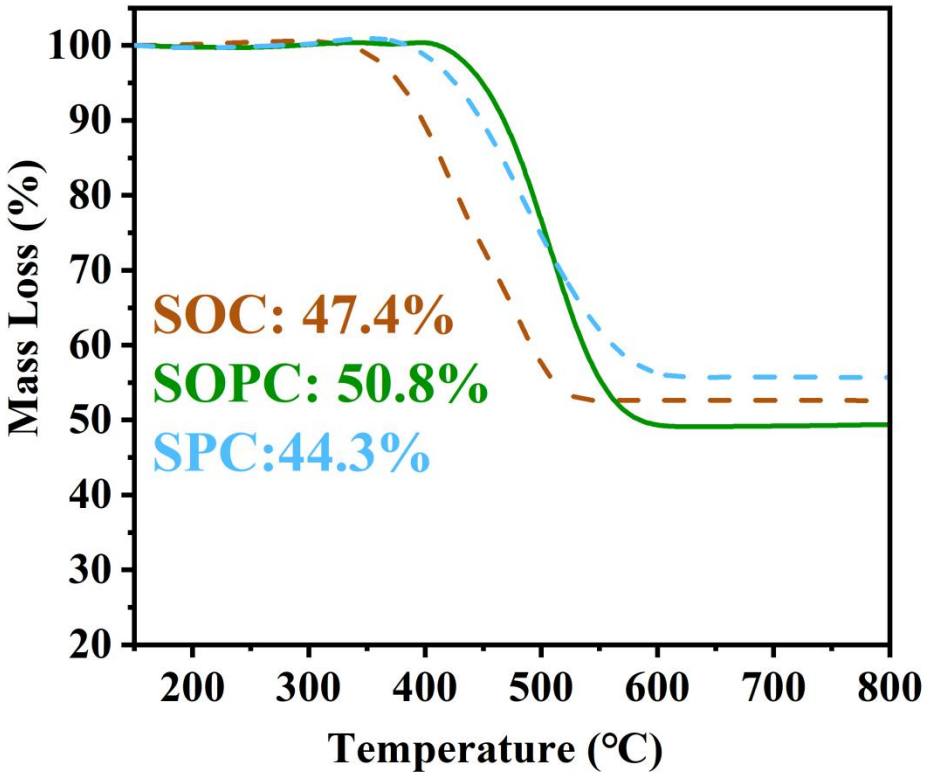

Fig. S1. TGA curve of SOC, SOPC, SPC.

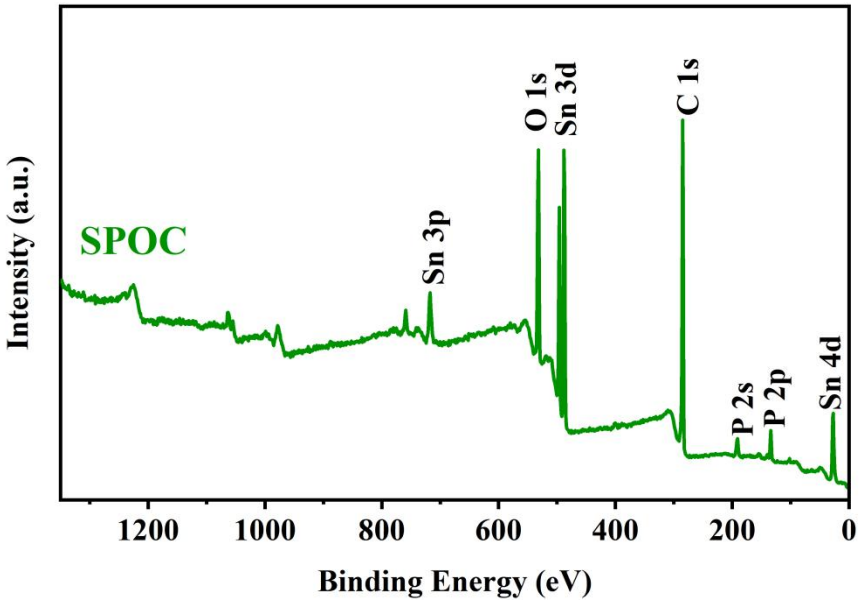

Fig. S2. XPS survey scan of SOPC.

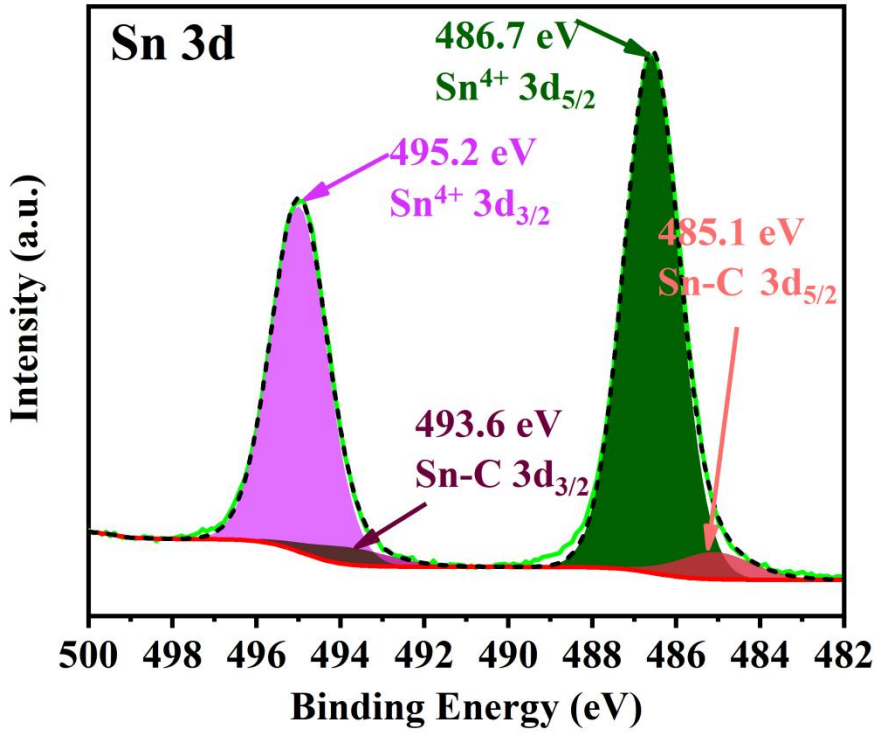

Fig. S3. XPS survey spectra of the Sn 3d region for SOPC

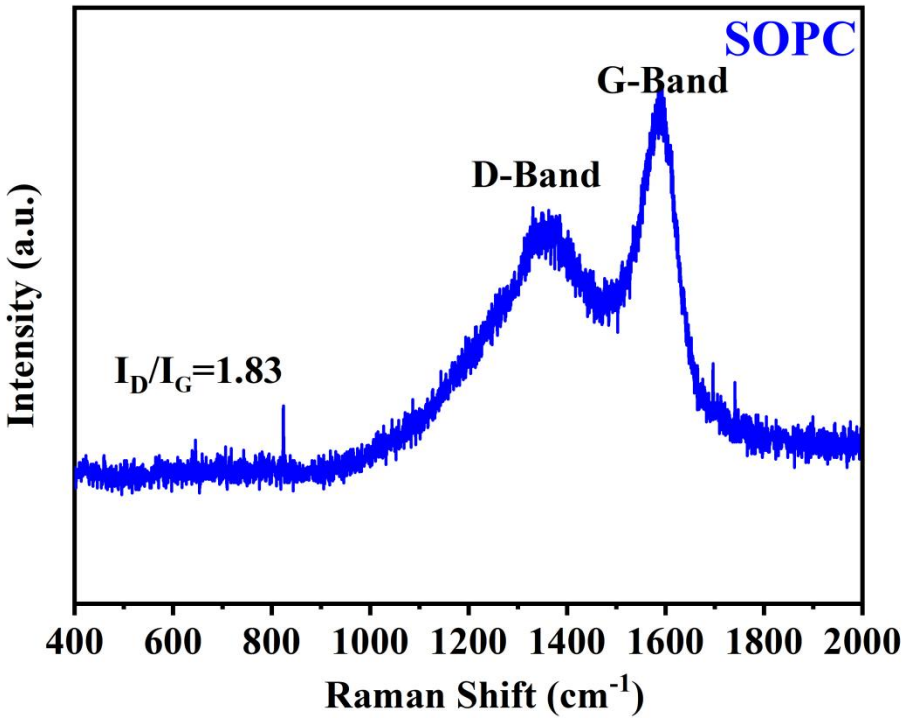

Fig. S4. Raman spectra of SOPC.

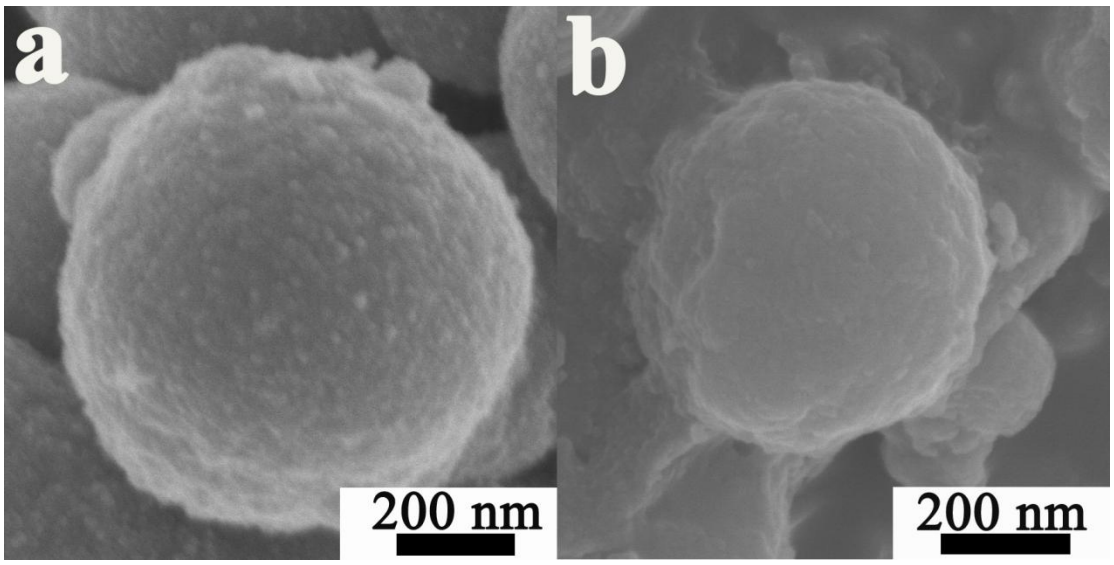

Fig. S5. SEM images of (a) SOC, (b) SPC.

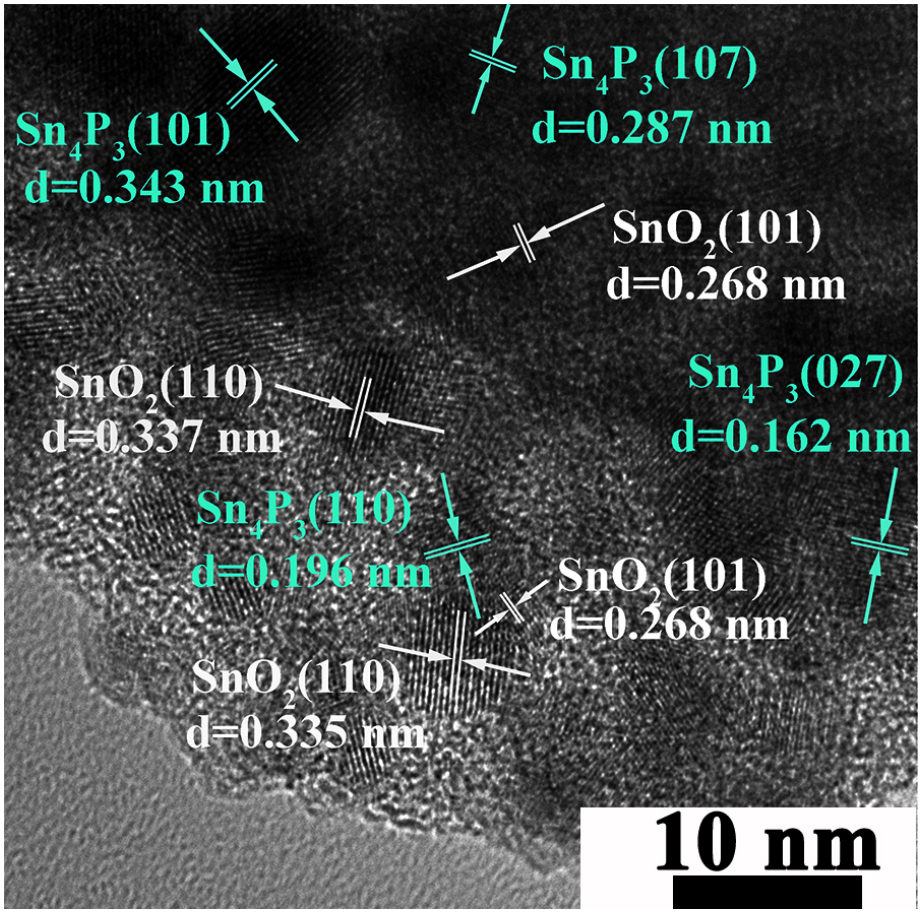

Fig. S6. HRTEM images of SOPC.

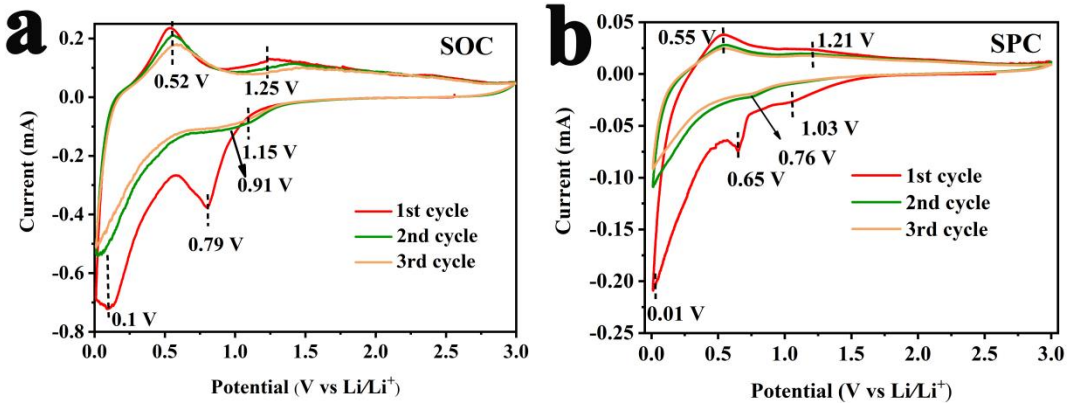

Fig. S7. CV curves of SOC and SPC at a scan rate of 0.1 mV s^{-1}.

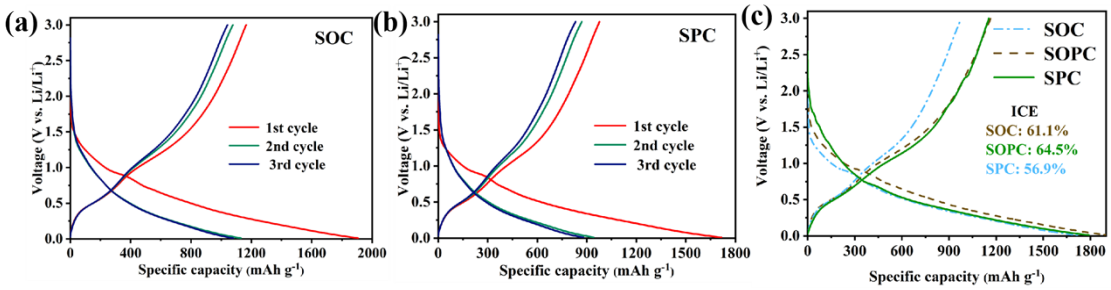

Fig. S8. The first charge/discharge cycle profiles of SOC、SOPC and SPC, The discharge/ charge profiles of (b) SOC and (c) SPC.

Table S1. Comparison the High-rate cycling performance of Sn-based anode electrodes for LIBs in recent years.

Anode	Current density ($A\ g^{-1}$)	Cycle number	Remaining capacity ($mAh\ g^{-1}$)	Ref
Sn_4P_3@MXene	1	300	847	[1]
C/Si@SnO_2	2	1000	330.4	[2]
	3	3000	262.54	
Sn/SnO_2@C	5	2000	508.2	[3]
SnO_2@C nanocage	1	600	792	[4]
	5	1000	477	
SnO_2@OMC	5	1000	321	[5]
SnO_2/Sn_4P_3@C	**1**	**500**	**901.5**	**This work**
	2	**800**	**739.8**	
	5	**1000**	**505.1**	
	10	**2000**	**224.2**	
	20	**3000**	**118.9**	
SnO_2@NC	1	1500	753	[6]
MWCNTs/Sn_4P_3@C	1	1000	569.5	[7]
Sn_4P_3-NC	1	400	507	[8]
SnO_2@MOF/graphene	1	1000	450	[9]
	2	1000	160	
Sn_4P_3/C	1	400	760	[10]

Reference:

[1] Fan, W.; Xue, J.; Wang, D.; Chen, Y.; Liu, H.; Xia, X. Sandwich-Structured Sn_4P_3@MXene Hybrid Anodes with High Initial Coulombic Efficiency for High-Rate Lithium-Ion Batteries. *ACS Appl. Mater. Interfaces* **2021**, *13* (51), 61055-61066.

[2] Liu, S.; Tao, W.; Yu, Y.; Fakudze, S.; Wang, C.; Wang, J.; Han, J.; Chen, J. Ball Milling Synthesis of Robust Sandwich-Structured C/Si@SnO_2 Anode with Porous Silicon Buffer Layer for Fast Charging Lithium-Ion Battery. *Colloids Surf., A* **2022**, *634*, 128976.

[3] Gao, S.; Wang, N.; Li, S.; Li, D.; Cui, Z.; Yue, G.; Liu, J.; Zhao, X.; Jiang, L.; Zhao, Y. Multi-Wall Sn/SnO_2@Carbon Hollow Nanofibers Anode Material for High-Rate and Long-Life Lithium-Ion Batteries. Angew. *Chem. Int. Ed.* **2021**, *60* (23), 12876-12884.

[4] Liu, M.; Fan, H.; Zhuo, O.; Chen, J.; Wu, Q.; Yang, L.; Peng, L.; Wang, X.; Che, R.; Hu, Z. A General Strategy to Construct Yolk-Shelled Metal Oxides Inside Carbon Nanocages for High-Stable

Lithium-Ion Battery Anodes. *Nano Energy* **2020**, *75*, 104368.
[5] Liu, D.; Wei, Z.; Liu, L.; Pan, H.; Duan, X.; Xia, L.; Zhong, B.; Wang, H.; Jia, D.; Zhou, Y. Ultrafine SnO_2 Anchored in Ordered Mesoporous Carbon Framework for Lithium Storage with High Capacity and Rate Capability. *Chem. Eng. J.* **2022**, *429*, 132185.
[6] Cheng, Y.; Wang, S.; Zhou, L.; Chang, L.; Liu, W.; Yin, D.; Yi, Z.; Wang, L. SnO_2 Quantum Dots: Rational Design to Achieve Highly Reversible Conversion Reaction and Stable Capacities for Lithium and Sodium Storage. *Small* **2020**, *16* (20), 2000681.
[7] Sun, S.; Li, R.; Wang, W.; Mu, D.; Liu, J.; Chen, T.; Tian, S.; Zhu, W.; Dai, C. One-Dimension Coaxial Cable-Like MWCNTs/Sn_4P_3 Materials with Long-Term Durability for Lithium Ion Batteries. Inorg. *Chem. Front.* **2020**, *7*, 3623-3632.
[8] Liu, Z.; Chen, J.; Fan, X.; Pan, Y.; Li, Y.; Ma, L.; Zhai, H.; Xu, L. Easy Encapsulation of Sn_4P_3 Nanoparticles into Honeycomb-Like Nitrogen-Doped Carbon Matrix with Enhanced Electrochemical Performance for Li-Ion Batteries. *J. Alloys Compd.* **2021**, *873*, 159836.
[9] Gao, C.; Jiang, Z.; Wang, P.; Jensen, L. R.; Zhang, Y.; Yue, Y. Optimized Assembling of MOF/SnO_2/Graphene Leads to Superior Anode for Lithium Ion Batteries. *Nano Energy* **2020**, *76*, 104868.
[10] Liu, Z.; Wang, X.; Wu, Z.; Yang, S.; Yang, S.; Chen, S.; Wu, X.; Chang, X.; Yang, P.; Zheng, J.; Li, X. Ultrafine Sn_4P_3 Nanocrystals from Chloride Reduction on Mechanically Activated Na Surface for Sodium/Lithium Ion Batteries. *Nano Res.* **2020**, *13* (12), 3274-3282.

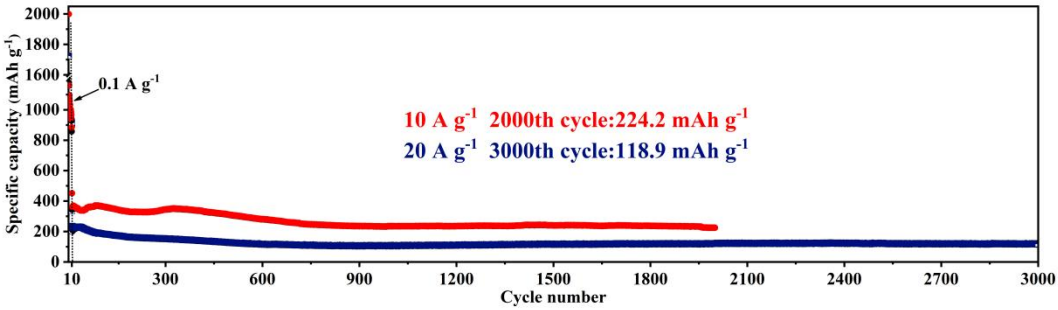

Fig. S9. Cycling performance of SOPC at 10A g^{-1} and 20A g^{-1}

Table S2. The charge capacity of SOC、 SOPC and SPC at the different cycles from the process of conversion reaction and alloying reaction, separately

Anode	Current density	Cycle number	Conversion reaction (Charge)/ (mAh g^{-1})	Alloying reaction (Charge)/ (mAh g^{-1})	Conversion reaction (Discharge)/ (mAh g^{-1})	Alloying reaction (Discharge)/ (mAh g^{-1})
SOC	1 A g^{-1}	50	35.3	565.9	329.1	268.7
		100	33.4	551.6	315.3	266.6
		200	31.3	550.3	322.2	258.1
		300	33.4	564.1	340.6	254.1
		400	41.6	582.2	365.9	256.3
		500	45.9	593.4	381.6	256.3
SOPC	1 A g^{-1}	50	91.7	532.9	368.3	252.9
		100	94.6	530	357.4	244.6
		200	108.3	565.8	421.7	247.1
		300	119.6	601.7	467.9	247.1
		400	144.6	690.4	550	277.9
		500	161.3	740.4	604.6	288.7
		600	175	780	650.8	294.6
SPC	1 A g^{-1}	50	30.5	237.3	171.9	94.5
		100	30.6	212	157.3	83.3
		200	33.3	251	186.5	94.5
		300	36.1	239	187.1	86.1
		400	36.1	214.5	174.6	75
		500	33.3	194.6	163.3	63.9

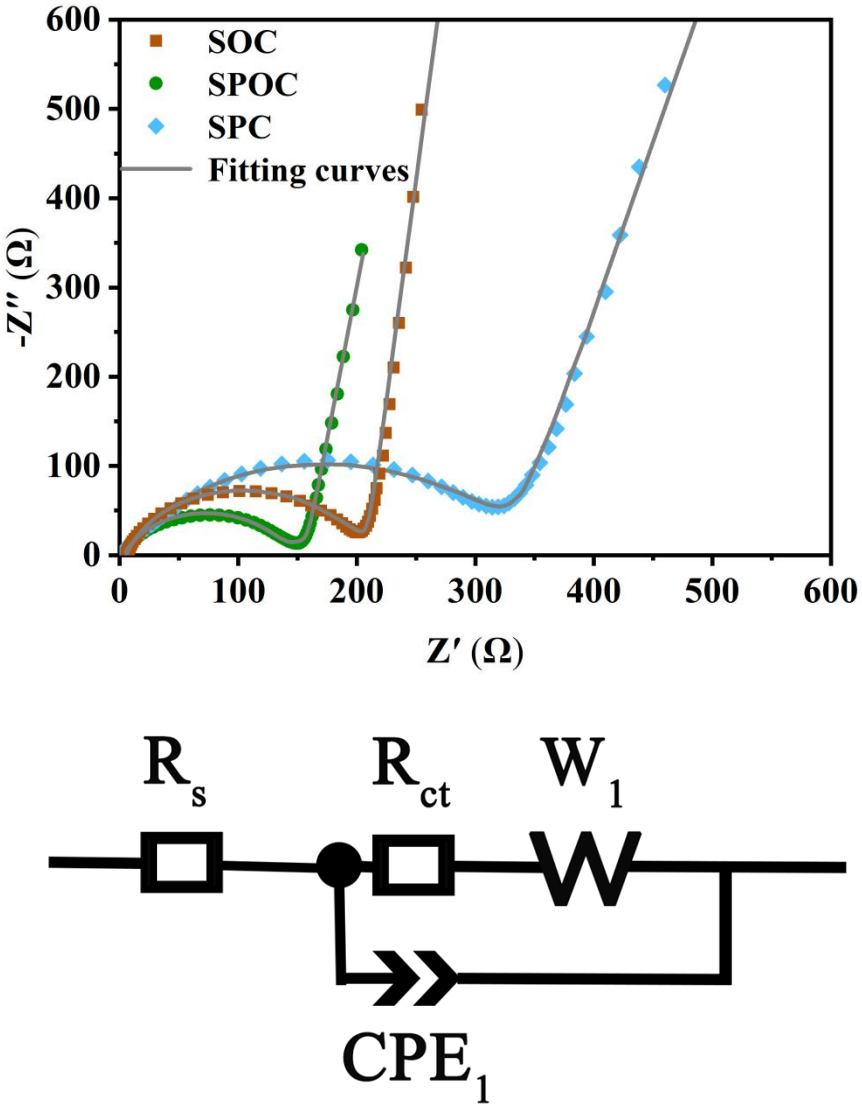

Fig. S10. EIS profifiles of SOC□SOPC and SPC electrodes at the fresh cell and the equivalent circuit for EIS fifitting.

Table S3. Rs and Rct value of SOC□SOPC and SPC electrodes before cycling

	SOC	SPOC	SPC
Rct（Ω）	189.9	135	320.3
Rs（Ω）	5.5	3.5	1.9

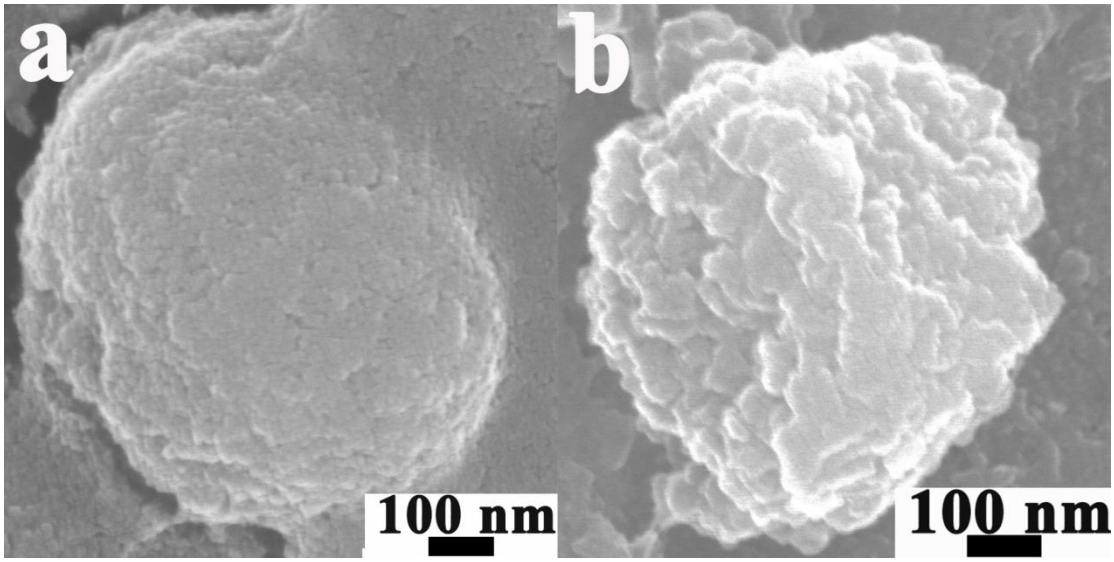

Fig. S11. SEM image of after 100 cycles of SOC and SPC cycle.

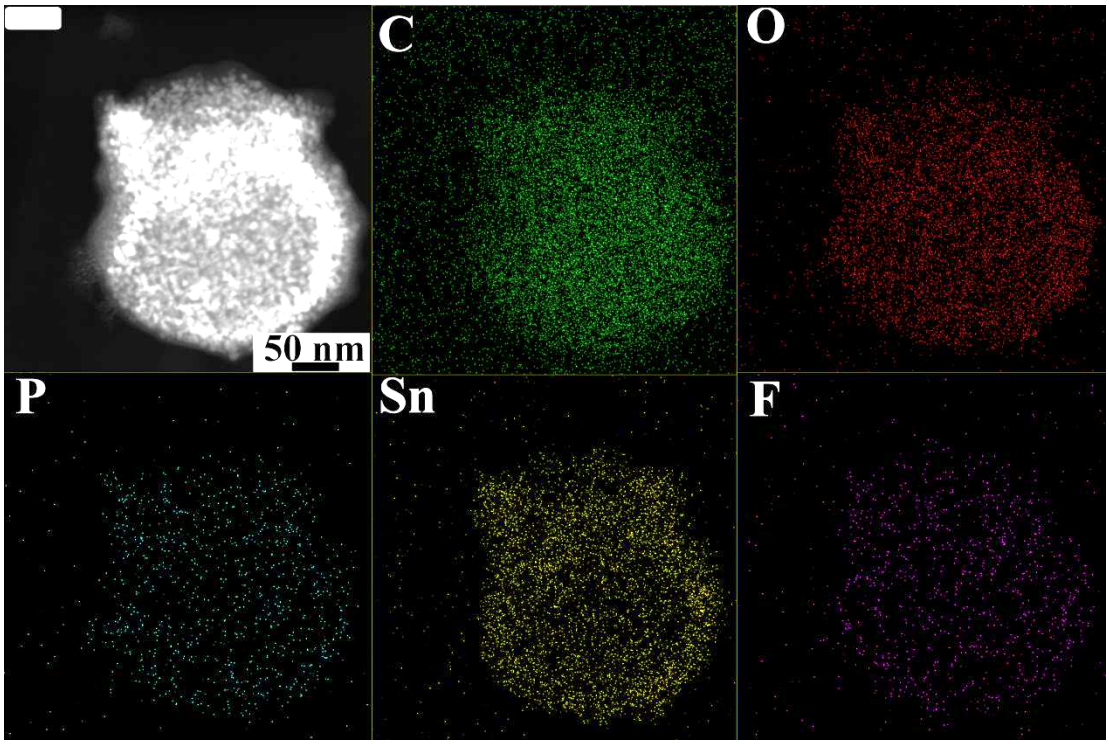

Fig. S12. EDX elemental mapping of C、O、P、Sn and F of SOPC of after 100 cycles of SOPC cycle.

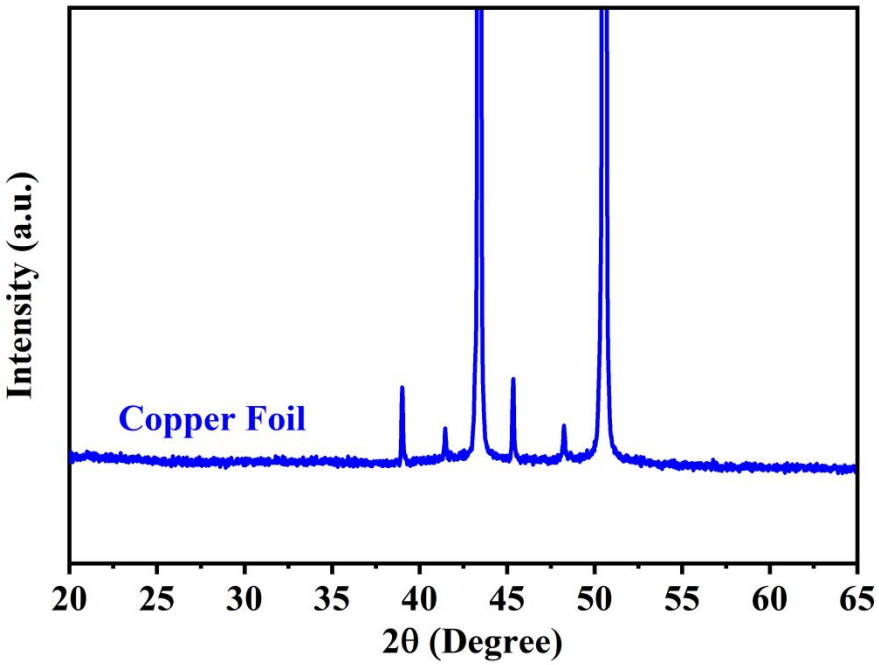

Fig. S13. XRD pattern of copper foil.

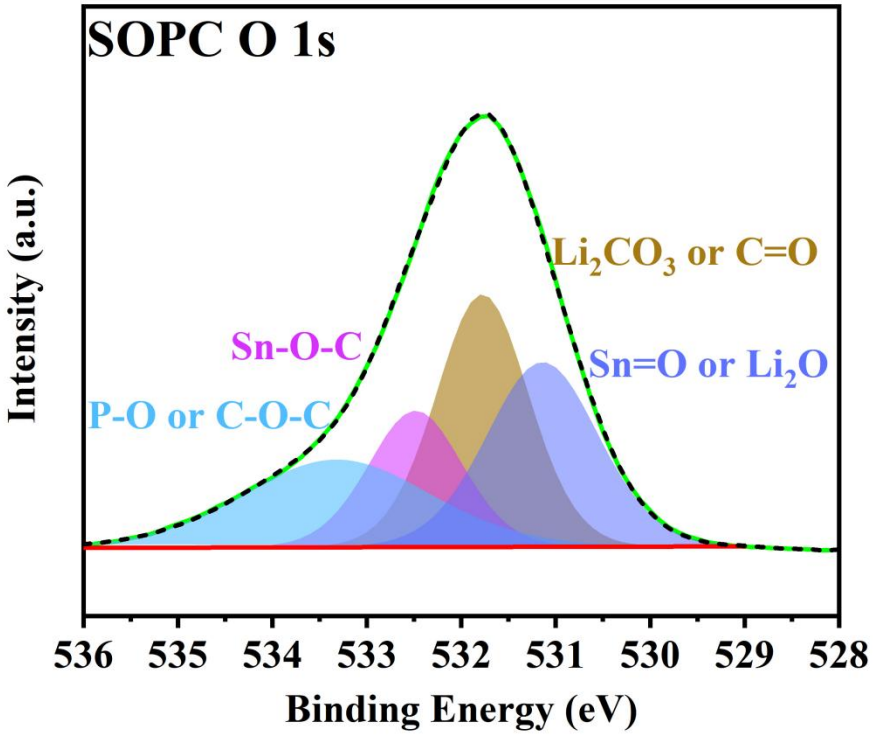

Fig. S14 XPS spectra of O 1s of SOPC after cycling .

Table S4. Calculated parameters for the energy level of SOC、SOPC and SPC.

Sample	Ecutoff (eV)	Eonset	WF (eV)
SOC	18.12	3.22	3.10
SOPC	18.31	3.28	2.91
SPC	17.65	3.09	3.57

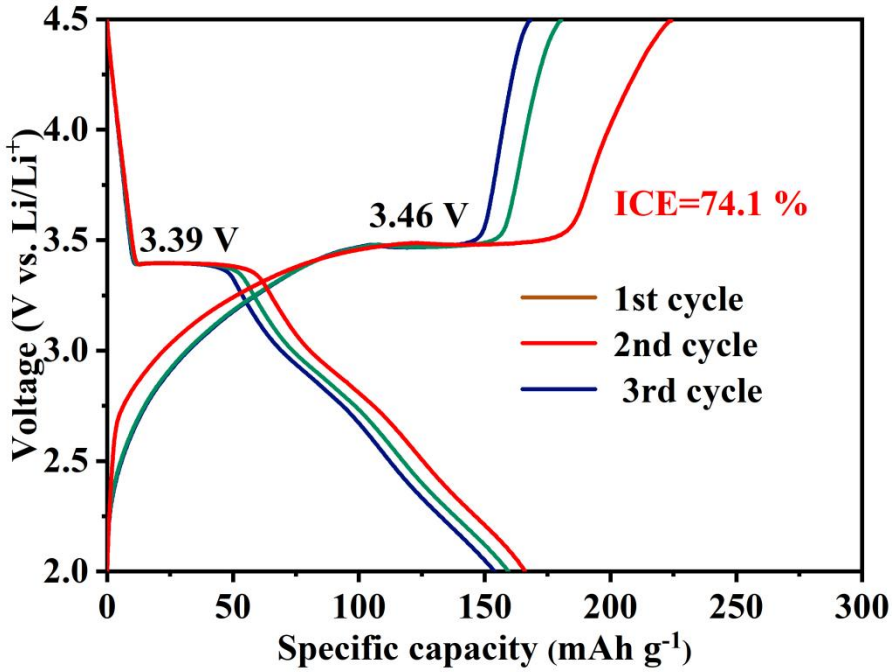

Fig. S15. The discharge/ charge profiles of SOPC||LPF full cell at 0.2 C